



Interfacing Circuit for two Galloping-based for two Galloping-based Piezoelectric Energy Harvester

Yuyin Chen, Dejan Vasic

► To cite this version:

Yuyin Chen, Dejan Vasic. Interfacing Circuit for two Galloping-based for two Galloping-based Piezoelectric Energy Harvester. IECON 2015 - 41st Annual Conference of the IEEE Industrial Electronics Society, Nov 2015, Yokohama, Japan. hal-01697547

HAL Id: hal-01697547

<https://hal.science/hal-01697547>

Submitted on 31 Jan 2018

HAL is a multi-disciplinary open access archive for the deposit and dissemination of scientific research documents, whether they are published or not. The documents may come from teaching and research institutions in France or abroad, or from public or private research centers.

L'archive ouverte pluridisciplinaire **HAL**, est destinée au dépôt et à la diffusion de documents scientifiques de niveau recherche, publiés ou non, émanant des établissements d'enseignement et de recherche français ou étrangers, des laboratoires publics ou privés.

Interfacing Circuit for two Galloping-based Piezoelectric Energy Harvester

Yuyin Chen

SATIE ENS Cachan

ENS Cachan

Cachan, France

yychen@ntumems.net

Dejan Vasic

SATIE ENS Cachan

Universite de Cergy-Pontoise

Cachan, France

vasic@satie.ens-cachan.fr

Abstract—In this paper a nonlinear interfacing circuit is examined to increase the power efficiency of multi galloping-based piezoelectric energy harvester. In the multiple flag structure application, the structure may be composed of many piezoelectric patches and the interfacing circuit becomes more complicated and important. An optimized synchronous electric charge extraction (OSECE) nonlinear technique is introduced to optimize the interfacing circuit. The equivalent circuit of the fluttering flags is introduced and simulated with the interface by using the Matlab and PSIM software. The experiment results show the good agreement with the theoretical analysis. The interfacing circuit design concept can be further used in the multi-piezoelectric patches energy harvesting system.

Keywords—Energy harvesting; piezoelectric; interfacing circuit; piezoelectric flag; fluttering.

I. INTRODUCTION

Energy harvesting from the ambient to provide the low power consumption device and microscale electronics become a practical and interesting topic during past decades. As piezoelectric materials are high power density, reliability and robustness, it becomes one of the most popular materials to be used in energy harvesting to transfer the vibration energy to electrical energy. Many researchers made efforts in developing energy harvesting devices from vibrations using cantilever beam based energy harvesters due to its simplicity and high efficient on generating large strain and power output [1-9]. Tang et al. [10] and Khaligh et al. [11] demonstrated the state of the art vibration piezoelectric energy harvesting setup based on simple cantilever beam design. Except vibrating-based energy harvester, wind force is also a good candidate to be the external energy force. O. Doaré, and S. Michelin propose the energy harvesting fluttering flexible plates in axial flow composed of many piezoelectric patches [12, 13]. Comparing to the fluttering flexible plates, galloping-based energy harvester is another type of wind-driven energy harvesting [14, 15]. The schematic of galloping piezoelectric energy harvester is shown in Fig 1. In classical cantilever beam based energy harvester, a nonlinear switching technique, the synchronized switching harvesting on inductor (SSHI) technique is a very successful and efficient technique to boost the piezoelectric output power [16-18]. These electric interfaces can be also applied to a galloping-based electric interface. Moreover, in the case of multi flags application, the structure may be composed of many piezoelectric patches and the interfacing circuit

becomes more complicated. Therefore, in this paper, we study an interfacing circuit applied at two flags working in galloping-based energy harvester application.

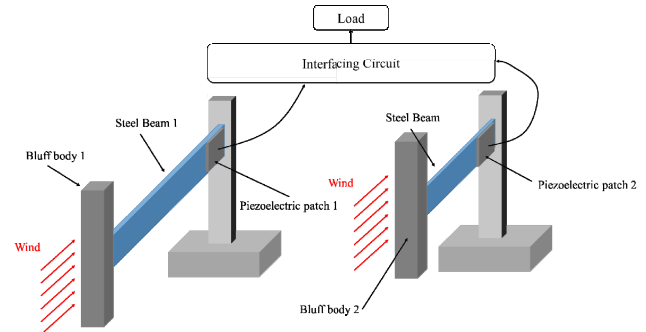


Fig. 1. Schematic of two galloping piezoelectric energy harvester with interfacing circuit to sing load.

Several interfacing circuit topologies and corresponding switching laws were proposed. The most efficient switching techniques can be classified into two groups according to the placement between the full-wave bridge rectifier and the switches. The first group of the switching circuits places the switches before the full-wave bridge rectifier, such as parallel-SSHI (Synchronized Switching Harvesting on an Inductor) the second group places the switches after the full-wave bridge rectifier, such as SECE technique [19]. Besides by using the full-bride to rectifier the piezoelectric voltage and in order to increase the efficiency, Wu et al. [20] propose the Optimized synchronous electric charge extraction (OSECE) technique as Figure 2. In this technique, a transformer and three diodes are instead of the inductor and full-bridge to rectifier the piezoelectric voltage and isolate the primary and secondary side. In these techniques, the switching circuit only turns “ON” at the extreme value of the displacement or at the zero crossing of velocity to shift the phase of the voltage across the piezoelectric element. These techniques are used because the piezoelectric-generator is weakly coupled to the host structure, i.e. only a small amount of mechanical energy is taken from the structure and converted in electricity. The electrical behavior of the piezoelectric-generator with the SSHI circuit is equivalent to an operation under strong coupling conditions by increasing the output voltage [21, 22].

To provide an interface for a multi flags energy-harvester, the interface called optimized synchronous electric charge extraction (OSECE) were used in this work. However the energy from each flag should be connected to one load, therefore we propose a new structure, which tries to connect the piezoelectric transducers working at different frequencies and different voltage amplitudes to one load. In order to study this new interface, in the next, an equivalent circuit of galloping piezoelectric energy harvester (GPEH) will be considered and combined with the interfacing circuit. The experiments will be compared to the simulation results (MATLAB+PSIM software) to show the performance in galloping-based applications. The paper is organized as follow: the second section summarizes the simulation of the two flags with electric interface. In section 3, the experimental results of the proposed electric interface with flags are presented. Finally, the last section concludes the paper.

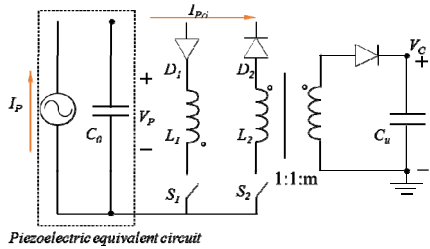


Fig. 2. Optimized synchronous electric charge extraction (OSECE).

II. THEORETICLA ANLYSIS

As shown in Fig 1, galloping-based energy harvester is composed of a bluff body placed at the tip of an elastic cantilever beam and piezoelectric patch placed at the fixed end of the beam. When an incoming facing wind flow through the bluff body and the beam, the wind will make beam to flutter and the strain will make piezoelectric patch transfer the mechanical energy to electrical energy. Considering the lumped parameter model and piezoelectric equations, the governing equations of the GPEH can be written as equation (1) [17].

$$\begin{cases} M\ddot{x}(L_b,t) + D\dot{x}(L_b,t) + K^E x(L_b,t) + \alpha V_p(t) = F_z(t) \\ F_z(t) = \frac{1}{2} \rho_a h L_{tip} U^2 C_{Fz} \\ I(t) = \alpha \dot{x}(L_b,t) - C_0 \dot{V}_p(t) \end{cases} \quad (1)$$

Where M , K_E , and D represent the effective mass, spring and damper of the system. $F_z(t)$, $V_p(t)$, $I(t)$ and $x(L_b, t)$ refer to external aerodynamic force, piezoelectric terminal voltage, piezoelectric output current and the displacement of the system. α and C_0 are the piezoelectric force-voltage coefficient and the clamped capacitor of the piezoelectric patch. L_b is the length of the cantilever beam, ρ is the air density, h is the edge length of the square section, L_{tip} is the length of the bluff body and U is

wind speed. C_{Fz} is the total aerodynamic force coefficient and it is a function of the angle of attack.

In order to use the governing equation into equivalent circuit model, the aerodynamic force can be further written as equation (2):

$$-\frac{1}{2} \rho_a h L_{tip} U^2 \left[\sum_{i=1,2,\dots} A_i \left(\frac{\dot{x}(t)}{U} + \beta \frac{V_c(t)}{K^E} \right)^i \right] \quad (2)$$

Combining the governing equation (1) and aerodynamic force equation (2), the equivalent circuit of GPEH is obtained as shown in Figure 3. The circuit consists of a static part, which is represented by the clamped capacitance C_0 , and a resonant branch which is corresponding to the first mechanical vibration mode. In the resonant branch, inductor L_m , resistor R_m and capacitor C_m are equivalent to the mass, the mechanical damping, and the stiffness of the first vibration mode respectively. The current i_1 flowing in the mechanical resonant branch is equivalent to the vibration velocity (dx/dt) of the actuating structure. The dielectric losses are neglected. The aerodynamical force F_z is obtained with a controlled voltage source that is a function of the voltage V_C at the capacitor C_m and the velocity i_1 .

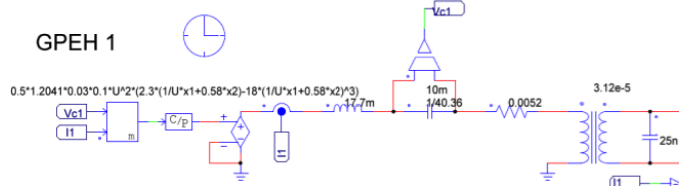


Fig. 3. Equivalent circuit of a galloping flag with piezoelectric patch.

In order to combine energy from two flags, the improved OSECE technique is introduced in this study (Fig. 4). In this structure there are 4 primary windings and 1 secondary winding transformer. As the conventional synchronized switching technique, the two switches are closed when the tip displacement reaches to the maxima value. The transformer in the OSECE is instead of the inductor in the synchronized switching technique to resonate with the clamped capacitor of the piezoelectric patch to withdraw the electrical energy from the piezoelectric patch and increase the output power.

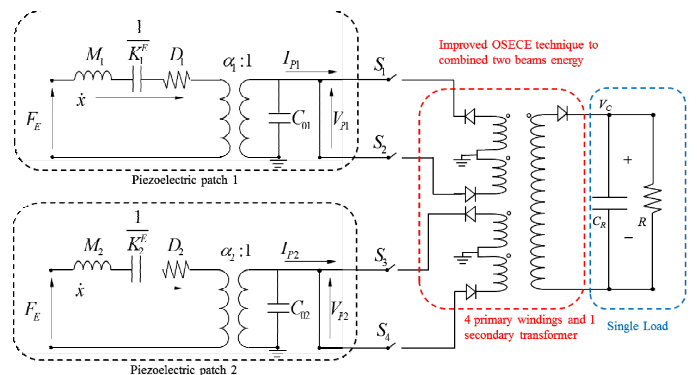


Fig. 4. Equivalent circuit of two galloping flags with proposed interfacing circuit.

The theoretical waveforms are shown in Fig. 5. In Fig. 5 we can see that the OSECE interface put in phase the piezoelectric voltage and the mechanical current that mean that this technique increase the output power. Moreover both flags contribute to charge the same output capacitance. The expression of the output power of OSECE technique is given in equation (3).

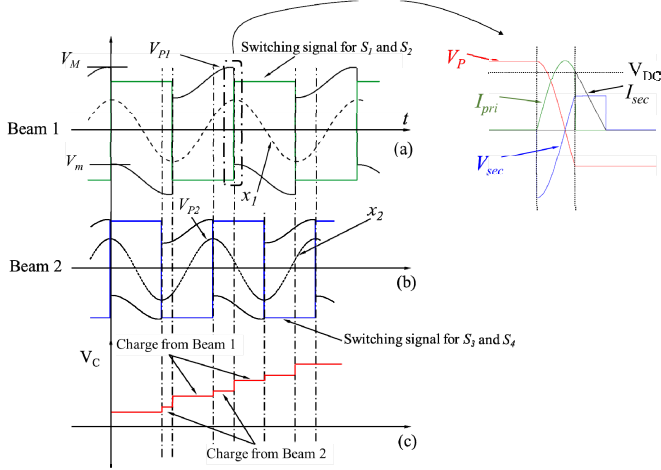


Fig. 5. Waveform of the OSECE technique.

$$\left\{ \begin{array}{l} P_{OSECE} = \frac{2\alpha^2\omega}{\pi C_0} \left[\frac{\sin^2(\omega_l t_m) e^{-\frac{\omega_l t_m}{Q_l}}}{1 + \cos(\omega_l t_m) e^{-\frac{\omega_l t_m}{Q_l}}} \right] x_M^2 \\ \omega_l t_m = \arctan(-m \sqrt{\frac{2\pi}{R_L C_0 \omega}}) + \pi \end{array} \right. \quad (3)$$

Where $\omega_l = \frac{1}{\sqrt{L_l C_0}}$ and $Q_l = \frac{1}{r_l} \sqrt{\frac{L_l}{C_0}}$ are the natural angular frequency and the quality factor for the LC resonance. m is the turn's ratio in the OSECE as shown in Figure 4. L_l , C_0 and r_l refer to inductance of the transformer in OSECE, clamped capacitance of piezoelectric patch and resistance of the LC resonance.

The electric equivalent circuit of the flag was implemented with the interfacing circuits OSCE in PSIM circuit simulator as shown in Fig. 6. The two flags where firstly simulated separately (GPH1 and GPH2), and then the two flags where combined with only one interface (GPH1+2) and charge the same load. The generated wind range is around 1m/s to 7 m/s.

The simulation results of the output power as function of the resistance load and the wind speed are plotted in 3D as shown in Fig. 7. Figure 7(a) shows the output power of the flag number 1. The maximum power is 133 μ W for a load 316 k Ω . Figure 7(b) shows the output power the flag number 2. The maximum power is 143 μ W for a load 316 k Ω . And the Figure 7(c) shows the output power of the combined two flag. The output power is 276 μ W. When the two flags are combined

with the OSECE to charge a single load, the load curve will not be changed and the optimal load is the same as the singe beam.

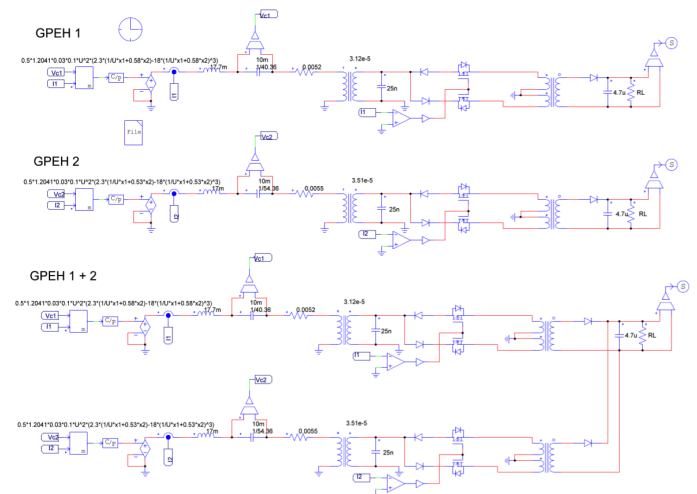
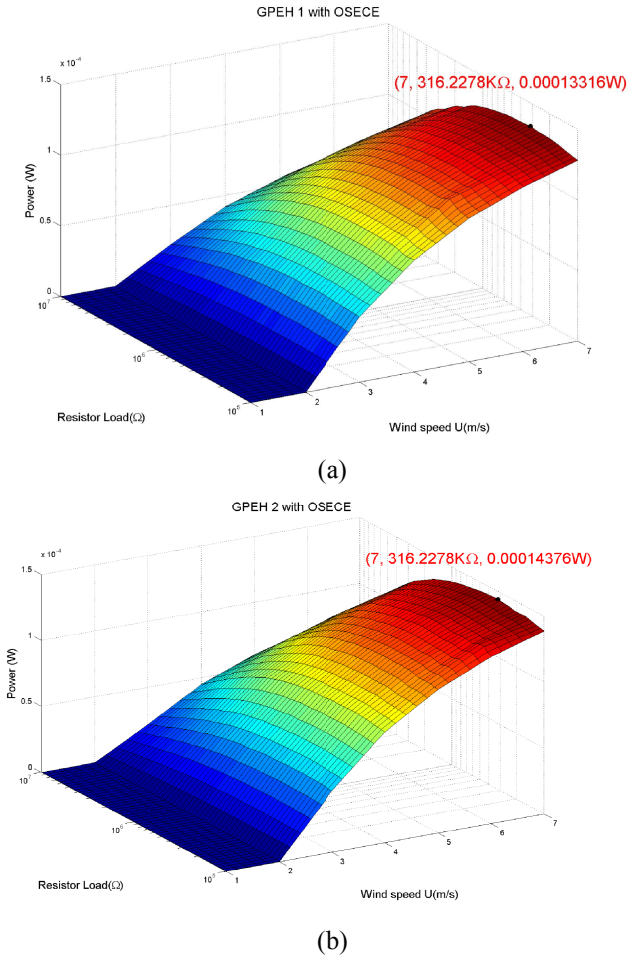


Fig. 6. Simulation setup in PSIM.



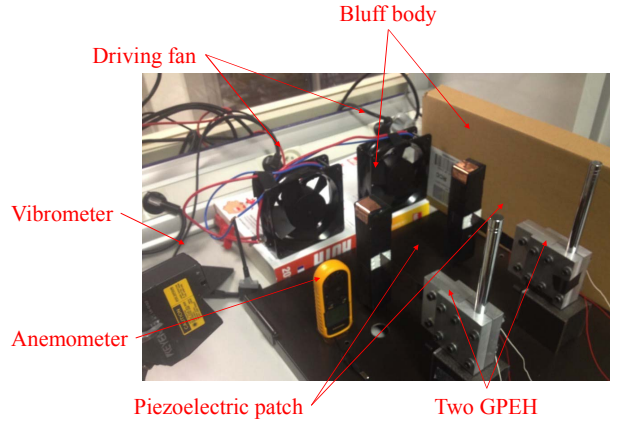
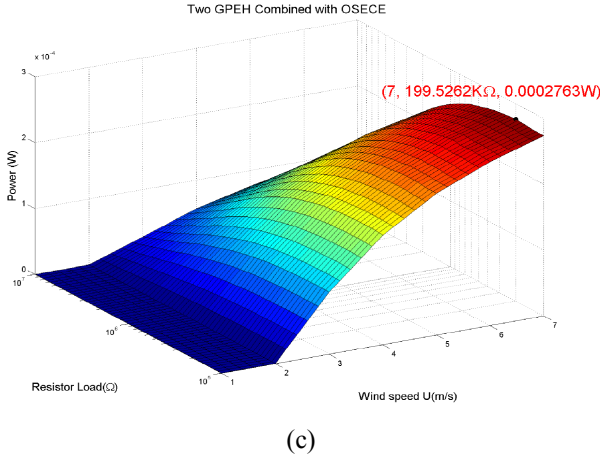


Fig. 7. Simulation results for (a)GPH 1 (b)GPEH 2 (c)GPEH 1+2.

III. EXPERIMENTAL SETUP AND RESULTS

The experimental setup and circuit photos are shown in Figure 8. Two galloping piezoelectric energy harvesters (GPEH) are placed on a steel plate and fixed by the magnetic clamer. A Laser vibrometer (LK-G152 and LK-G3001P, KEYENCE) is place on the right side of the GPEH to measure the tip displacement. The external wind source is driven by two fans (4184 NXH) and the wind speed U can be controlled by a DC power supply from 12-28 VDC. The generated wind range is around 1.5 m/s to 6 m/s. Two GPEHs are driven by two fans simultaneously and, through two combined OSECE interfacing circuit, the harvested energy from two piezoelectric patches charge a single load. Two diodes, one transformer and two switches are used in each OSECE interfacing circuit as Figure 8 shown. The model of diodes are BAT48 and the voltage drop is around 0.22V. The model of transformer is PT8SM. There are two windings in primary side and one winding in the secondary side. The turn's ratio is 1:1.2 and the inductance is around 10 mH. The output rectifier capacitor is 4.7 μ F. The dimensions of steel beams, piezoelectric patches and bluff bodies are shown in Table 1. The model parameters of the two GPEHs are shown in Tables 2 and 3. Two different length GPHEs are used here to show the performance of the combined OSECE.

TABLE I. DIMENSIONS OF THE GPEH AND PIEZOELECTRIC PATCHES

Symbol	Value (unit)
Steel Beam 1	120*20*0.5 (mm^3)
Piezoelectric patch 1	20*14*0.3 (mm^3)
Bluff body 1	100*30*30 (mm^3)
Steel Beam 2	110*20*0.5 (mm^3)
Piezoelectric patch 2	20*14*0.3 (mm^3)
Bluff body 2	100*30*30 (mm^3)

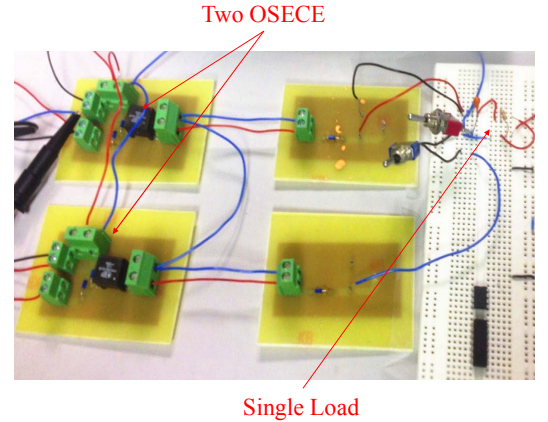


Fig. 8. Experimental setup and interfacing circuits..

TABLE II. MODEL PARAMETERS OF GPEH 1.

Symbol	Description	Value (unit)
M_1	Mass	17.7 (g)
f^{op}_1	Open circuit resonant frequency	7.6 (Hz)
f^{sh}_1	Short circuit resonant frequency	7.57 (Hz)
k^2_1	Electromechanical coupling coefficient	0.0079
K^D_1	Equivalent stiffness when piezoelectric patch is in open circuit	40.36 (N/m)
K^E_1	Equivalent stiffness when piezoelectric patch is in short circuit	40.04 (N/m)
D_1	Damping coefficient	0.0052 (N/m/s)
α_1	Force-voltage factor	0.0000312 (N/V)
C_{01}	Clamped capacitance of piezoelectric patch	25nF

TABLE III. MODEL PARAMETERS OF GPEH 2.

Symbol	Description	Value (unit)
M_2	Mass	17 (g)
f_{op}^2	Open circuit resonant frequency	9 (Hz)
f_{sh}^2	Short circuit resonant frequency	8.97 (Hz)
k^2_2	Electromechanical coupling coefficient	0.0067
K^D_2	Equivalent stiffness when piezoelectric patch is in open circuit	54.36 (N/m)
K^E_2	Equivalent stiffness when piezoelectric patch is in short circuit	54 (N/m)
D_2	Damping coefficient	0.0055 (N/m/s)
a_2	Force-voltage factor	0.0000351 (N/V)
C_{02}	Clamped capacitance of piezoelectric patch	25nF

The experimental waveforms of the piezoelectric voltage s(channel 1 and 3) of each flag (V_{P1} and V_{P2}) and the output DC voltage V_C (channel 2) are shown in Figure 9. The two piezoelectric voltages are diphase because of the different size of the flag. But these two voltages charge the same capacitor without any interference.

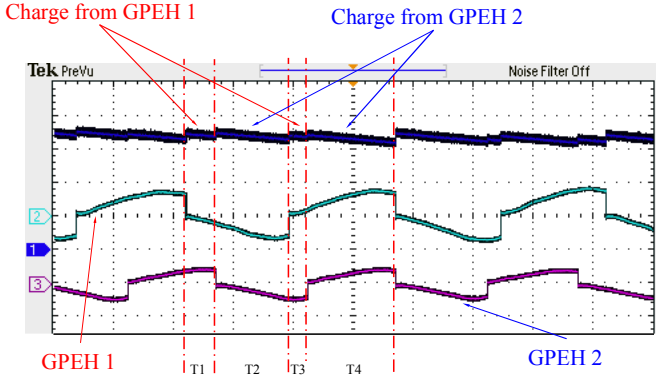


Fig. 9. Experimental waveform: channel 1 V_c (10V/div), channel 2 V_{p1} (20V/div), and channel 3 V_{p2} (20V/div)

The experimental results for three wind speed U are shown in Fig. 10. The black, blue and red curves present the simulation results of GPEH1, GPEH2 and the combined GPEH1+2 from MATLAB+PSIM. The black curve with circle dots, blue curve with square dots and red curve with star dots present the experimental results. With the wind speed increasing, the power output of three circuits will also increase. Comparing the experimental results to simulation results, the experimental power is lower than The main reason for the losses between the experimental and simulation results is because in the simulation the ideal transformer is used and in the experiments there are losses when the transformer stored and transfer the electrical energy simulation and because a part of harvested energy is used to drive switches. The maximum experimental power of the combined structure is $160 \mu\text{W}$ for a wind speed of 5m/s and respectively $75 \mu\text{W}$ and $80 \mu\text{W}$ for each beam separately. That means that the proposed improved OSECE can combine the energy provided by each beam whiteout interference.

The optimal load for the three cases are almost the same. Moreover in the OSECE technique, the optimal load range is wider than in classical synchronized switching technique harvesting in inductor (SSH). The output power during the resistor load range up to $1 \text{M}\Omega$ is almost a flat curve. The results also shows that by using OSECE technique to combine two flags to a single load the optimal load will not be changed. This technique will not influence the load response curve. It means that whole system is load independent and this result shows good agreement with the simulation results.

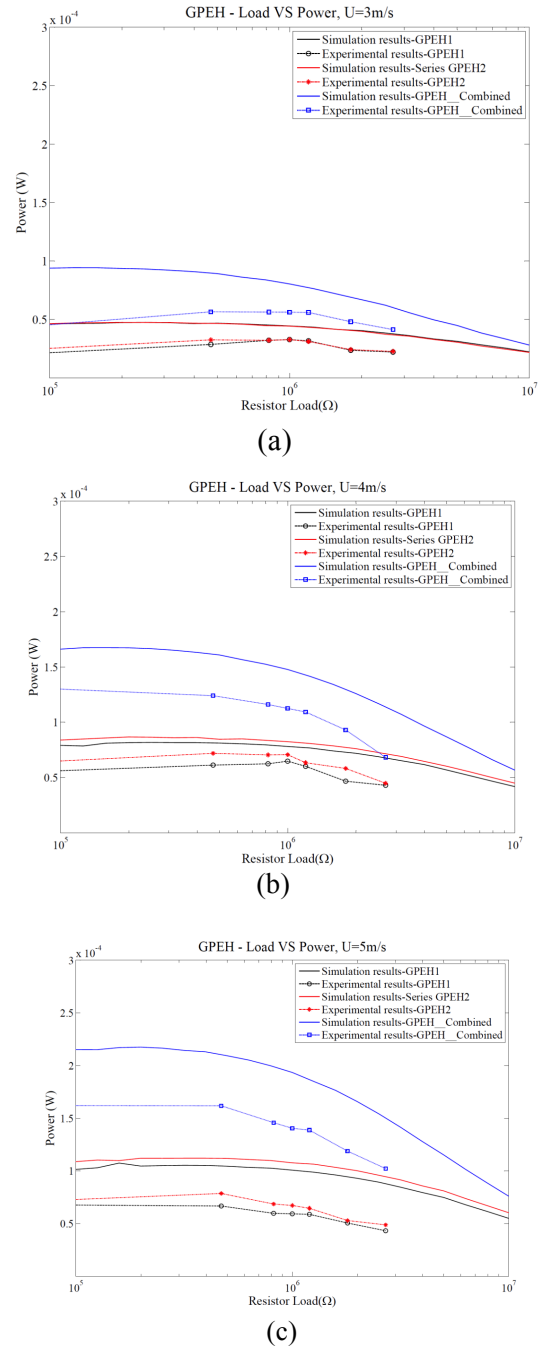


Fig. 10. Experimental and simulation results in different wind speed (a) $U=3\text{m/s}$ (b) $U=4\text{m/s}$ (c) $U=5\text{m/s}$.

IV. CONCLUSION

In this study, an electric interface (OSECE) is proposed to connect two piezoelectric beams with only one load. Experimental results verify the simulation results by MATLAB and PSIM software. In the load response testing (driven at each resonance), OSECE technique with two beams show low dependence on load effect. The wide optimal load range is an advantage in real application and for multi-piezoelectric system. The two beams combined system will not influence the load curve for each piezo patch. In the case of variation of the wind speed, the two beams combined system show good performance to plus electrical energy and will not influence for each piezo patch either.

The two beams system proposed in this study is the simplest system in the multi-piezoelectric patches system. The results show that the combined technique can be used in multi-piezoelectric patch system and plus the electrical energy without influencing the load curve and frequency response. This advantage is important to different piezoelectric patches and different structure design applications. As the piezoelectric flag energy harvesting application, the whole system can be composed of many piezoelectric patches and only load need to be charge.

ACKNOWLEDGMENT

The authors are grateful to Eleceram Technology co. ltd. The funding of this project, from Agence Nationale de la Recherche, France under ANR FLUTTENER project, is gratefully acknowledged.

REFERENCES

- [1] H. A. Sodano, et al., "A review of power harvesting from vibration using piezoelectric materials" vol. 36. Thousand Oaks, CA, USA: Sage, 2004.
- [2] S. Roundy, "On the effectiveness of vibration-based energy harvesting," Journal of Intelligent Material Systems and Structures, vol. 16, pp. 809-823, Oct 2005.
- [3] E. Lefeuvre, et al., "Piezoelectric energy harvesting device optimization by synchronous electric charge extraction," Journal of Intelligent Material Systems and Structures, vol. 16, pp. 865-876, Oct 2005.
- [4] D. Guyomar, et al., "Toward energy harvesting using active materials and conversion improvement by nonlinear processing," IEEE Trans. Ultrason. Ferroelectr. Freq. Control, vol. 52, pp. 584-595, 2005.
- [5] E. Lefeuvre, et al., "A comparison between several approaches of piezoelectric energy harvesting," Journal De Physique Iv, vol. 128, pp. 177-186, 2005.
- [6] M. Lallart, et al, "Double synchronized switch harvesting (DSSH): A new energy harvesting scheme for efficient energy extraction," IEEE Trans. Ultrason. Ferroelectr. Freq. Control, vol. 55, pp. 2119-2130, 2008.
- [7] S. Roundy and P.K. Wright, "A piezoelectric vibration based generator for wireless electronics," Smart Materials & Structures, vol. 13, pp. 1131-1142, Oct 2004.
- [8] T.H. Ng and W.H. Liao, "Sensitivity analysis and energy harvesting for a self-powered piezoelectric sensor," Journal of Intelligent Material Systems and Structures, vol. 16, pp. 785-797, Oct 2005.
- [9] S. Kim, W. W. Clark, and Q.-M. Wang, "Piezoelectric Energy Harvesting with a Clamped Circular Plate: Analysis," Journal of Intelligent Material Systems and Structures, vol. 16, pp. 847-854, Oct 2005.
- [10] L. Tang, Y. Yang and C.K. Soh (2010) Toward broadband vibration-based energy harvesting. Journal of Intelligent Material Systems and Structures 21: 1867-1897.
- [11] A. Khaligh, P. Zeng and C. Zheng (2010) "Kinetic energy harvesting using piezoelectric and electromagnetic technologies—state of the art." IEEE Transactions on Industrial Electronics 57(3): 850-860.
- [12] O. Doaré, and S. Michelin, "Piezoelectric coupling in energy-harvesting fluttering flexible plates: linear stability analysis and conversion efficiency." Journal of Fluids and Structures 27.8 (2011): 1357-1375.
- [13] S. Michelin, and O. Doaré, "Energy harvesting efficiency of piezoelectric flags in axial flows." Journal of Fluid Mechanics 714 (2013): 489-504.
- [14] L. Tang, L. Zhao, Y. Yang, E. Lefeuvre, "Equivalent Circuit Representation and Analysis of Galloping-Based Wind Energy Harvesting," Mechatronics, IEEE/ASME Transactions on, vol.20, no.2, pp.834,844, April 2015.
- [15] L. Zhao, L. Tang, and Y. Yang. "Synchronized charge extraction in galloping piezoelectric energy harvesting." Journal of Intelligent Material Systems and Structures (2015): 1045389X15571384.
- [16] Y.Y. Chen, D. Vasic, F. Costa, C.K. Lee, W.J. Wu, Self-Powered Semi-Passive Piezoelectric Structural Damping Based on Zero Velocity Crossing Detection. Smart Materials & Structures, Volume 22, Issue 2, 025029, February 2013
- [17] Y.Y. Chen, D. Vasic, Y.P. Liu, F. Costa, Study of a Piezoelectric Switching Circuits for Energy Harvesting with Bistable Broadband Technique by Work-cycle Analysis. Journal of Intelligent Materials Systems & Structures, Volume 24, Issue 2, pp. 180-193, January 2013
- [18] Y. Y. Chen, et al., "A self-powered switching circuit for piezoelectric energy harvesting with velocity control," European Physical Journal-Applied Physics, vol. 57, 3090, Feb 2012.
- [19] E. Lefeuvre, A. Badel, C. Richard, and D. Guyomar, "High performance piezoelectric vibration energy reclamations," Smart Structures and Materials 2004: Smart Structures and Integrated Systems, vol. 5390, pp. 379-387, 2004.
- [20] Y. Wu, A. Badel, F. Formosa, et al., Piezoelectric vibration energy harvesting by optimized synchronous electric charge extraction. Journal of Intelligent Material Systems and Structures 24(12): 1445-1458, 2012.
- [21] Y. C. Shu, I. C. Lien, and W. J. Wu, "An improved analysis of the SSHI interface in piezoelectric energy harvesting," Smart Materials & Structures, vol. 16, pp. 2253-2264, Dec 2007.
- [22] H. Wu, L. Tang, Y. Yang, and C.K. Soh, 2013, "A Novel Two-Degrees-of-Freedom Piezoelectric Energy Harvester," J. Intell. Mater. Syst. Struct., 24(3), pp. 357-368.